Supplementary Material
A novel family of non-parametric cumulative based divergences for point processes

Sohan Seth
University of Florida

Il "Memming" Park
University of Texas at Austin

Austin J. Brockmeier
University of Florida

Mulugeta Semework
SUNY Downstate Medical Center

John Choi, Joseph T. Francis
SUNY Downstate Medical Center & NYU-Poly

José C. Príncipe
University of Florida

A Optimal stimulation parameter selection

A.1 Method

The data used in this analysis is from a single chronically implanted rat with two 16-channel tungsten micro-wire arrays (Tucker Davis). Neuronal activity was recorded from arrays in S1 and in ventral posterolateral nucleus (VPL) of the thalamus using the Plexon Multichannel Acquisition Processor. Action potentials were detected using a constant threshold and were sorted by a semi-automated clustering procedure (SortClient) using the first 3 principal components of the detected waveforms.

Prior to each recording session, anesthesia was induced by isofluorane followed by a Nembutal injection and maintained with isofluorane. Neurons with receptive fields in the arm/hand region were identified audibly and by delivering a short thwack using a mechanical tactor that lightly contacted the first digit on the rats right paw at 2Hz for 120s, yielding 240 presentations.

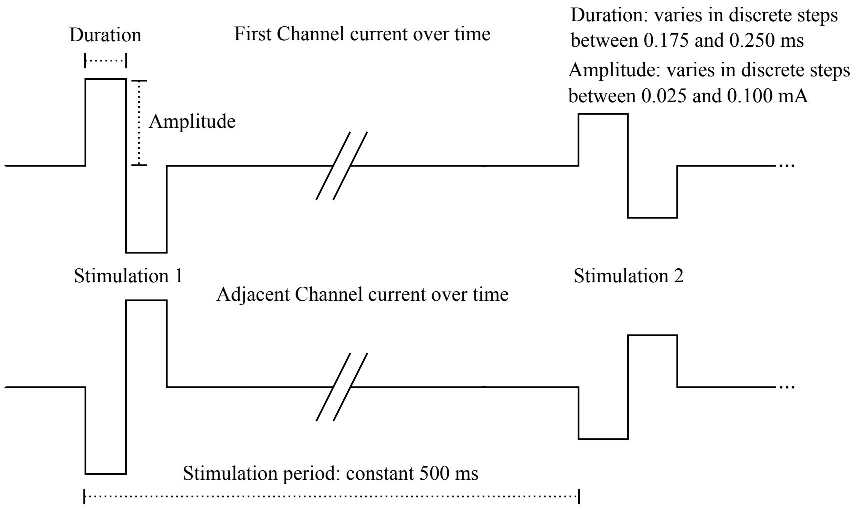

Figure 1: Waveforms for stimulating channels.

Bipolar microstimulation (AM Systems Model 2200 Isolator) was then applied to two adjacent electrodes that corresponded to neurons with strong activity in response to the tactile stimulation. Each stimulation consisted of a biphasic squared pulse, see Figure 1. The pulse duration and current amplitude was varied, but the stimulations were always at 500 ms apart. During each session, 19 distinct pairs of pulse duration and current amplitude were applied, with 140 responses from each pair randomly permuted throughout the recording. Thus the goal was to compare the 240 natural touch responses to the 140 microstimulation responses from each parameter variation.

In order to compare the temporal response, the tactile and electrical stimulation needed to be aligned. A difficulty with microstimulation is that the produced artifact prevents recording for nearly 6 ms on the entire array. The corresponding initial 6 ms response on each trial to tactile touch was removed. A window of 40 ms was used for comparison. The firing rate returned to an equilibrium level by the end of the window as in figure 2.

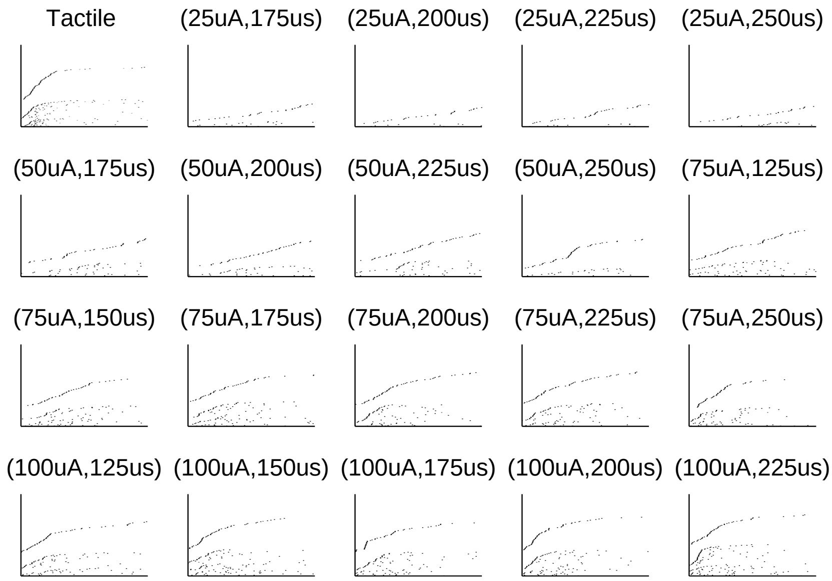

Figure 2: Response pattern from tactile input and all electrical stimulation parameter settings that were scanned. Time is shown on the x-axis between 0 and 40ms. The y-axis shows trials sorted by number of spikes than first spike time. This plotting shows the count distribution and spike timing for all realizations.

B Extra hypothesis testing results

B.1 Poisson process

Poisson process is the simplest, and perhaps, the most widely used point process model. We test if the proposed methods can detect difference in the rate profile while maintaining the average rate constant. In Poisson process, the count distribution has variance equal to the mean rate, hence for higher rates the data becomes sparsely spread among the dimensions Ω_n. For this example of rate 3, 90% of the count distribution is concentrated in the range of one to seven spikes.

Since the rate function fully describes this process, the performance of the rate based statistic λ_{L2} is the best in this case (see Figure 3). Also since the count distribution for H_0 and H_1 are identically Poisson distributed, Wilcoxon test (denoted N) fails to detect the difference. K-S and C-M based divergences performs similarly, yet it is interesting to note that C-M is consistently better than the K-S divergence.

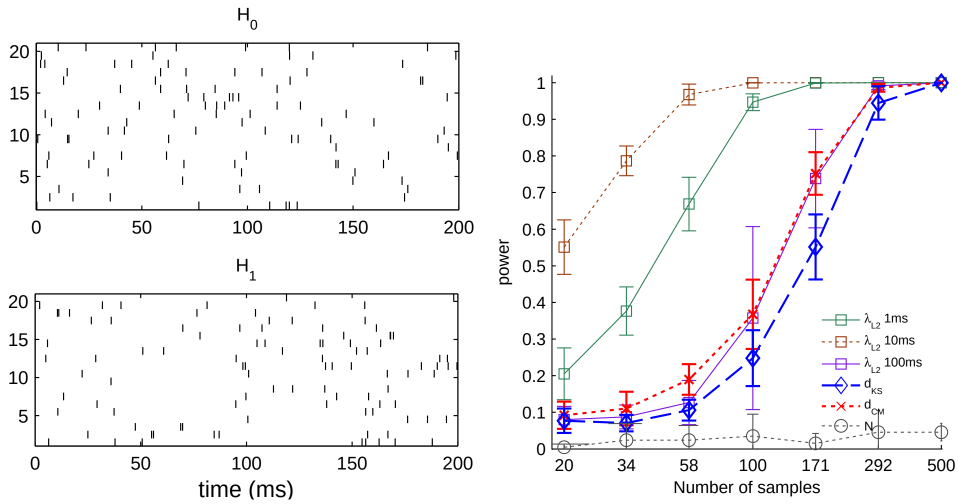

Figure 3: Poisson process. (Left) Spike trains from the null and alternate hypothesis. The rate function is constant during each 100 ms interval. The rate of H_0 changes from 20 to 10 spk/s, and for H_1 it changes from 10 to 20 spk/s. (Right) Comparison of the power of each method. The Wilcoxon test on mean count (labeled with N) stays around the threshold level (0.05). All other methods are empirically consistent for this example. The error bars are standard deviation over 10 Monte Carlo runs.

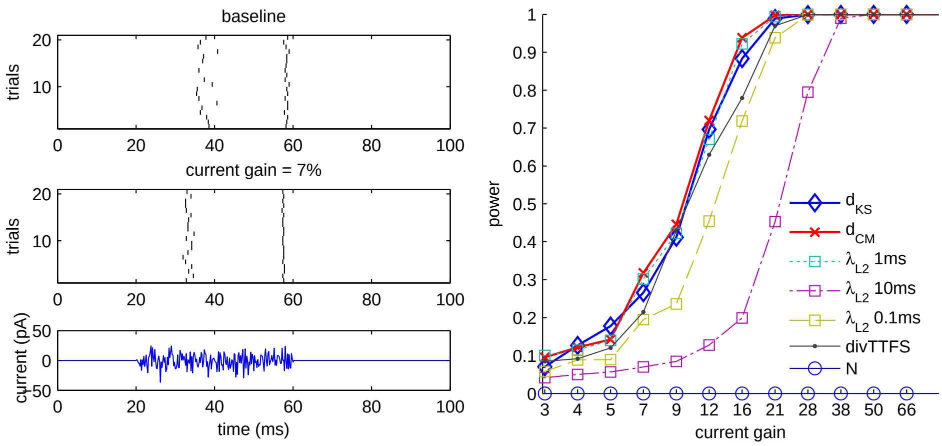

Figure 4: Izhikevich neuron model. (Left) example spike trains from the model for the baseline current (top) and with increased gain (middle). The bottom trace is the waveform of the injected current. (Right) Comparison of the power of each method for different input scaling. TTFS is the K-S statistic for the jitter distribution of the time to first spike.

B.2 Neuron model

We investigate the sensitivity of the proposed methods in a neurophysiological scenario. We simulated a repeated injection of current to a neuron model, and observed the output spike train pattern. By varying the gain factor of input, we investigate the sensitivity of various statistics to a realistic statistical change. Izhikevich's simplified neuron model for Class 2 neuron is stimulated with noisy current injection [1, Ch 8]. The dynamics of the model is fully described by the following equations,

$$\begin{aligned} \dot{v} &= 0.04(v+42)(v+82) & \qquad \text{if } v \geq 30, \text{then} \\ \dot{u} &= 0.2(0.26v - u) & v \leftarrow -65 \end{aligned}$$

where spike times are recorded whenever v is reset. Frozen noise is generated from white Gaussian wave form with duration 40 ms. The noise is injected to the neuron model with additional noise current that is generated for each trial. The neuron model is sensitive to certain feature of the noise [2], hence precisely timed action potentials are observed (see Figure 4). When the frozen noise was scaled up, the action potentials generally reduced their variance and fired in earlier time on average (see Figure 4).

The input current is adjusted such that 2 action potentials are generated on average. The sample size is 30 spike trains for each condition. The C-M and K-S measures both perform at least as good as the best rate based measure. Additionally, a K-S test on the jitter distribution to the first event (time to first spike), ignoring the second spike timing, is compared and shown to be slightly worse than the proposed method.

B.3 Serial correlation model

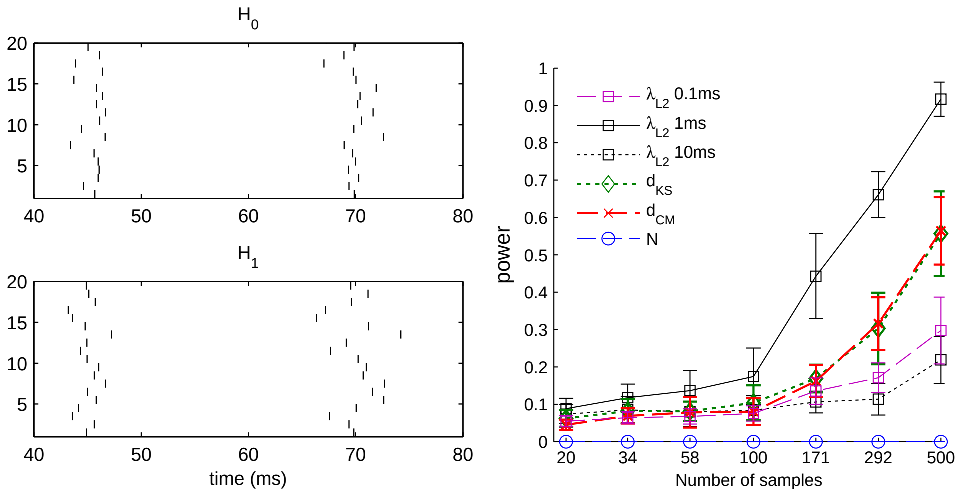

Figure 5: Renewal process with (H_0) or without serial correlation (H_1). (Left) Spike trains from the null and alternate hypothesis. (Right) Comparison of the power of each method. The error bars are standard deviation over 10 Monte Carlo runs.

Serial correlation in point process is defined by the autocovariance of the intervals (time between spikes). Due to internal dynamics of neurons, the spike trains can have serial correlation [3]. We simulated a renewal process without serial correlation and a point process with same marginal interval distribution but with a non-zero serial correlation [4]. We restrict our problem to two intervals only, where each interval distribution is a convolution of two uniform distributions.

It turns out this problem is quite difficult and hundreds of samples are needed to discriminate them (see Figure 5). Both K-S and C-M type tests perform equally well, while the Wilcoxon test fails to differentiate between the two point processes. An optimized kernel size for the rate function statistic outperforms both K-S and C-M type test.

References

[1] E. M. Izhikevich. *Dynamical systems in neuroscience : the geometry of excitability and bursting*. Computational Neuroscience. MIT Press, 2007.

[2] Z. F. Mainen and T. J. Sejnowski. Reliability of spike timing in neocortical neurons. *Science*, 268(5216):1503–1506, 1995.

[3] F. Farkhooi, M. F. Strube-Bloss, and M. P. Nawrot. Serial correlation in neural spike trains: Experimental evidence, stochastic modeling, and single neuron variability. *Physical Review E (Statistical, Nonlinear, and Soft Matter Physics)*, 79(2):021905+, 2009.

[4] M. J. Chacron, B. Lindner, and A. Longtin. Noise shaping by interval correlations increases information transfer. *Physical Review Letters*, 92(8):080601+, 2004.